Transition Structures for D-Ribulose-1,5-bisphosphate Carboxylase/Oxygenase-Catalyzed Oxygenation Chemistry: Role of Carbamylated Lysine in a Model Magnesium Coordination Sphere

Mónica Oliva, Vicent S. Safont, and Juan Andrés*

Departament de Ciències Experimentals, Universitat Jaume I, Box 224, 12080 Castelló, Spain

O. Tapia†

Department of Physical Chemistry, Uppsala University, Box 532, S-75121 Uppsala, Sweden

Received: November 27, 2000; In Final Form: February 14, 2001

The oxygenation chemistry catalyzed by D-ribulose-1,5-bisphosphate carboxylase/oxygenase (Rubisco) is theoretically characterized with transition structures (T-Ss) describing enolization, oxygen fixation, hydration, and concerted O−O and C2−C3 bond breaking. These T-Ss are obtained at HF/3-21G, HF/6-31G**, and B3LYP/6-31G** levels of theory. Hydroxypropanone models the substrate embedded in the Mg coordination shell including a model of the carbamylated lysine. The enolization transition vector describes the intramolecular hydrogen transfer from C3 to the carbonyl oxygen (O2). The carbamylated lysine shows a striking catalytic effect by modulating the dihedral angle of the fragment O2−C2−C3−O3. For the isolated hydroxypropanone, the angle is ca. −5°, decreasing to ca. −60° in the Mg-embedded model. The torsion diminishes the hydroxypropanone singlet−triplet energy gap and prompts the interaction with $^3O_2$. In turn, an intersystem crossing channel is opened along the reaction path. The lowest energy T-S for oxygen fixation is a spin singlet with a hydroxyperoxy structure; the precursor describes activated oxygen (peroxide) hydrogen-bonded to H−O3. The best electronic description of the hydrogen shuttling in both transition structures is via homolytic bond breaking/forming processes. For hydration, the transition structure leads to a *gem*-diol at C3. The final step is a concerted O−O and C2−C3 bond rupture, represented by a six-center transition structure. It describes the simultaneous hydrogen shuttling from one O−H of the *gem*-diol (O3−H) to the hydrogenated oxygen of the peroxy function to form water, and the bond ruptures. The resultant water molecule is directly located in the first coordination shell of magnesium. The successor complex in this step represents the products of the global chemistry. Once they leave, the Mg active site would be ready to go for a new catalytic run, which is the hallmark of an enzyme. It is therefore most encouraging to find it as a result of the present model; thus, one of the gas oxygen atoms is transformed into a solvent molecule and the other is incorporated in the model glycolate moiety in agreement with experiment. The model correlates well with hydrogen and oxygen isotope labeling experimental results. According to our model, no Michaelis complex is necessary as O_2 binds to form a precursor complex via intersystem crossing with the successor complex of the enolization step.

Introduction

An enzyme usually selectively catalyzes a one-step chemical conversion process helped by a multistep molecular mechanism related to substrate binding and product release.[1] Rubisco, D-ribulose-1,5-bisphosphate carboxylase/oxygenase, is an exception as it cannot distinguish between oxygen and carbon dioxide attack on to the substrate D-ribulose-1,5-bisphosphate (RuBP); moreover, it can catalyze self-inhibition reactions.[2−4] Rubisco is recognized to be one of the key enzymes in the carbon metabolism of plants,[5] because it catalyzes the initial step in the photosynthetic CO_2 fixation to RuBP, yielding two molecules of 3-phospho-D-glycerate (3-PGA). RuBP is then regenerated in the Calvin cycle, and the fixed carbon is incorporated into carbohydrates. Rubisco also catalyzes a competing oxygenase reaction of the substrate, thus leading to a loss of energy by photorespiration. In this reaction, O_2 instead of CO_2 is added to RuBP, yielding 3-PGA and 2-phosphoglycolate (2-PG). The latter is metabolized in the glycolate pathway, which produces CO_2 and dissipates energy as heat. The net efficiency of the photosynthesis is reduced by up to 50% for this photorespiratory pathway, depending upon the relative concentration of CO_2 and O_2.[5−14] An improvement of the biomass production would require photorespiration to be repressed as much as possible. It is understandable that a genetic redesign of Rubisco aiming at increasing the discrimination power between CO_2 against O_2 is still attracting much interest. A theoretical explanation of such mechanistic complexity, then, is not only an important issue in biochemistry and theoretical physical chemistry but also a challenge that any theory on enzyme catalysis must confront.

The products of the oxygenation chemistry, 3-PGA and 2-PG,[5,15] are obtained via enolization of the substrate RuBP, followed by oxygen fixation at the C2 center (cf. Figure 1 for atom numbering). This would lead to an oxyperoxy intermediate, to which a water molecule would be incorporated, forming a

† Visiting Iberdrola Professor.
* To whom correspondence should be addressed.

10.1021/jp004287y CCC: $20.00 © 2001 American Chemical Society
Published on Web 04/21/2001

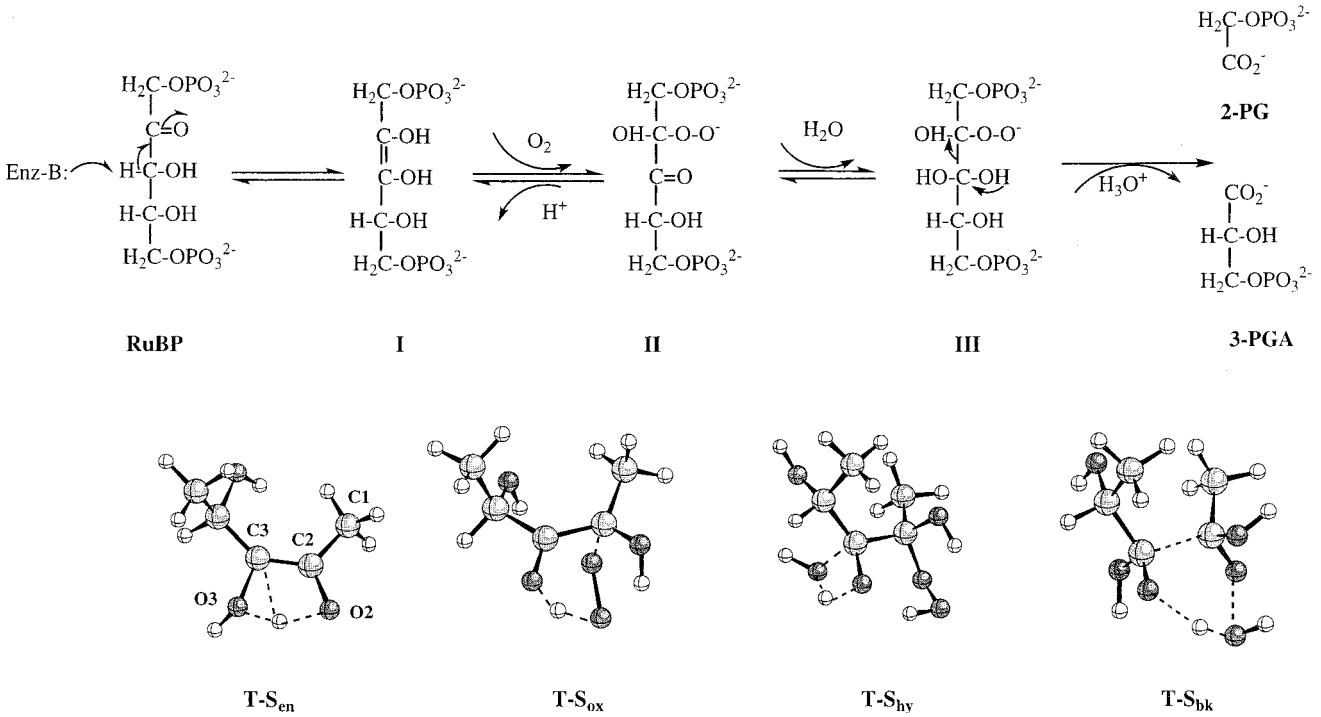

Figure 1. Reaction pathway for the oxygenation of RuBP catalized by Rubisco, extracted from Hartman and Harpel[14] and adapted by us in the upper row. The second row represents the five-carbon T-Ss for the oxygenation chemistry.[37] Atom numbering is indicated.

gem-diol at the C3 center. Thereafter, the C2−C3 and O−O bonds must be broken and one oxygen atom from O_2 should form a water molecule and the other remains fixed to C2 in a carbonyl function. Rubisco is capable of catalyzing the whole set of reactions one after another[14,16] at the same active site.

RuBP and the corresponding product molecules are in the singlet ground electronic state.[15,17] However, the gas substrate enters the reaction in the spin triplet ground electronic state. In absence of an external magnetic field gradient, the spin projection along an arbitrary direction (M_S) is conserved. Rubisco has no magnetic centers so that only the $M_S = 0$ would participate in the chemistry. Therefore, the enzyme, somehow, has to help achieving an intersystem crossing. This is one of the issues addressed here. To add more complexity to the mechanistic scenario, at the same active site, carbon dioxide binds at the C2 center, followed by a sequence of chemical steps similar to those described above, including now a configuration inversion at C2 center since the products are two 3-PGA.[18]

There is little doubt that such a mechanistic complexity shown by Rubisco stands as a challenge to quantum theorists and physical chemists. A successful theoretical description should explain not only the chemistry catalyzed by the wild type but also the changes shown by a variety of mutants. In a larger perspective, solving the inevitability riddle[19] (e.g., once the RuBP-enzyme is activated, oxygenation or carboxylation cannot be avoided if the corresponding gas substrate is at the active site) may possibly yield hints on general principles of enzyme catalysis.

Pauling, in 1948, noted that the active site of an enzyme should be complementary in shape to the activated complex of the reaction to be catalyzed.[20] The first theoretically determined "activated complex" having a shape complementary to the active site was identified for the hydride-transfer step in liver alcohol dehydrogenase.[21] An X-ray structure [22] and the theoretical transition structure in a vacuum were docked so that only the transition structure (T-S) geometry, but not the reactants or the products, could be located without steric hindrances inside the active site.[21,23] The conclusion reached at that point concerned the substrates: the enzyme must mold the reactants as much as possible into the geometry of the saddle point. In this perspective, one of the factors prompting for catalysis would be determined by destabilizing the reactants so that the energy gap with the T-S is decreased.

The theoretical study of enzyme catalyzed reactions is following three lines of development. One, illustrated by Kollman and co-workers[24] and Lightstone et al.,[25] was originated in the pioneering work by Warshel and Levitt.[26,27] A structure−function relationship is quantitatively determined by using the system's 3D structure to model a free energy along putative reaction pathways. A second line, followed in our group, focus on the molecular mechanism by directly identifying T-Ss obtained as saddle points of index one that are compatible with the active site of the corresponding enzyme.[21] The transition structure approach is complementary to the methods using full structural information in molecular dynamics simulations. The basic idea in our method is that a transition structure geometry and its transition vector is a property of the reactant system having key elements invariant to molecular perturbations represented by the protein.[21,28] A third approach that can integrate these two lines of thinking has been developed by Williams and co-workers[29,30] where the Hessian can be diagonalized and the nature of the saddle points can be established in the presence of the enzyme. The partitioning of the reactant system into a quantum and a classical subsystem was early proposed by one of us.[31−33] With appropriate internal coordinates, the Hessian can be partitioned in different subsystem contributions.[34] This approach was used to justify the invariance of the transition structure toward interactions with nonresonant modes belonging to the medium (solvent and/or protein). Actual calculations became possible with the program GRACE.[29,30] Upon application of this method to Rubisco, the transition structure invariance in the carboxylation step has been documented.[35] This result shows that studies of the kind reported by us have a bearing on the real system.

The discovery of a minimal molecular model (MMM) of RuBP sustaining the full chemistry in absence of the enzyme provides a unique starting point.[36,37] For now, the introduction of selected features from the enzyme can be used to sense differential effects that could be interpreted as catalytic effects. RuBP has been modeled with a three-carbon (3-C)[36,38] and a five-carbon (5-C)[28,37,39] frame including the ketone group at C2 and the alcohol function at C3 at different levels of theory. Here, the MMM is used to examine the differential effects produced by a model magnesium coordination sphere. A preliminary report on enolization and oxygenation transition structures has recently been published.[40] Here we report a comparison with different levels of electronic theory; besides HF/3-21G, full characterizations with HF/6-31G** and B3LYP/6-31G** density functional approach are reported.

Model, Theory, and Computations

Hydroxypropanone is the MMM of the substrate RuBP. The model gave adequate qualitative answers in the sense that the C-framework found in the T-Ss shares the geometric disposition of more complex models.[4,28,34,36−39,41]

On the basis of X-ray crystallographic data (particularly from spinach),[42] a model mimicking the active site was constructed. Magnesium was included in the calculations, and its coordination sphere was modeled by carbamate (carbamylated ammonia), representing the carbamylated Lys 201, two formates (Asp 203 and Glu 204), a water molecule, and hydroxypropanone. One hydrogen atom in each model side chain is fixed in order to keep the coordination sphere around the magnesium center as if it were in the protein. This is the only geometric constraint imposed to our model. In this way, the active-site residues adapt their orientation and conformation to the changes of the reacting substrates.

The strategy followed to obtain the T-S starts searching a saddle point directly in the quadratic zone of the energy hypersurface. The exact characterization of such stationary structures[43,44] is achieved by using a simple algorithm.[34,45,46] The coordinates describing the system are separated into two sets: the control space, which is responsible for the unique negative eigenvalue in the respective force constant matrix,[47] and the remaining coordinates, referred to as complementary space. The geometry optimizations are carried out alternatively on each subspace, one at a time, until the stationary structure is obtained. Examination of the T-Ss is achieved by the evaluation of the Hessian matrix; the number of negative eigenvalues defines the type of saddle point (index). Once the stationary points are obtained, the transition vector is related to the imaginary eigenvalue. This T-S conveys two types of information. One yields, at zero order, very concisely the essentials of the chemical process under study.[47,48] A second type of information is given by a calculation of normal modes.

From the stationary T-Ss one can define precursor and successor complexes. For hydrogen transfer, characteristic of the reported T-Ss, the precursor geometry belongs to the saddle point except for the hydrogen that is optimized in the direction of reactants. In other words, the substrate is molded into the geometry of the T-S. The successor has the T-S geometry, except for the hydrogen optimized at the acceptor center. The precursor and successor complexes can only exist at active sites of enzymes as transient structures.

The stationary points were located by optimizing the geometry at HF/3-21G and HF/6-31G** basis sets and density functional theory calculations at B3LYP/6-31G**. Berny analytical gradient optimization routines were used.[49,50] The density matrix converged to within 10^{-9} au; the threshold value of maximum displacement and maximum force were 0.0018 Å and 0.00045 hartree/bohr. All calculations were carried out with the GAUSSIAN 94[51] and GAUSSIAN 98[52] programs. Supplementary vibration and spectral analysis is produced with the GaussView[53] package.

Oxygenation Chemistry

Experimentally, the oxygen fixation mechanism has been developed following the pattern of carbon dioxide fixation mechanism. Aside from the carbamylation step, the chemistry is portrayed in Figure 1.

The first conclusive work on the mechanism established that one of the oxygen atoms (from molecular oxygen, O_2) was incorporated to the carboxylic group of 2-PG,[19] thereby implying an O−O bond breaking. The second oxygen is lost to the medium as a water molecule. Furthermore, from water molecules initially present at the active site, an oxygen atom is incorporated into 3-PGA. A first mechanistic scheme was proposed[19] involving a peroxide intermediate. This molecule incorporates a water molecule, yielding another intermediate that suffers C−C bond breaking and a final dehydration to give the products (Figure 1).

Several aspects of the oxygenation chemistry have to be taken into account. They are as follows: (1) Lorimer's inevitability postulate[19] indicated that the binding site of Rubisco, once activated for carboxylation, was also activated for oxygenation. (2) How does the enzyme discriminate between CO_2 and O_2? This issue was not clear, although, from the electronic viewpoint, our previous work[54,55] identified a possible source of intersystem crossing which differs from the standard carbanion description.[18] (3) A carboxyketone intermediate of the carboxylase reaction was isolated, prompting the postulate of a corresponding peroxyketone intermediate in the oxygenase reaction.[16,56] (4) Mutants at the position of Lys 334[56] (Lys 329 in the *Rhodospirillum rubrum* sequence) are nearly devoid of carboxylation activity. Moreover, a novel O_2-dependent side product was identified for these mutant enzymes as 2-carboxytetritol 1,4-bisphosphate (CTBP). This product seems to verify the formation of a hydroperoxide intermediate. (5) Rubisco must stabilize the peroxy intermediate for efficient cleavage of the C2−C3 and peroxyl O−O bonds. Such stabilization would avoid pathways other than production of 3-PGA and 2-PG that predominate with wild-type Rubisco. In mutant enzymes, however, the peroxide intermediate would be destabilized, yielding hydrogen peroxide and CTBP.[56]

It is obvious that the complexity described above cannot be rationalized with a model missing all molecular features in the enzyme. Notwithstanding, the existence of the set of transition structures calculated with the 3-C and 5-C models nicely correlates with the above mechanism;[37] the T-Ss for the 5-C model are reported in the second row of Figure 1. First, the molecular model sustains all the intramolecular redox chemistry via intramolecular hydrogen shuttling. Second, the structural results can be compared to the work pioneered by Andersson, Brändén, and Schneider.[5,42] The structural data confirm that the global geometry of the T-Ss is complementary in shape to the active site of Rubisco. Thus, one knows, by construction, that the geometry of the T-S is not determined by the protein structure. They are stationary species on their own. The question now is to determine whether such species are robust when the model includes elements of the active site. If the answer is positive, one may have a chance to gauge catalytic effects on

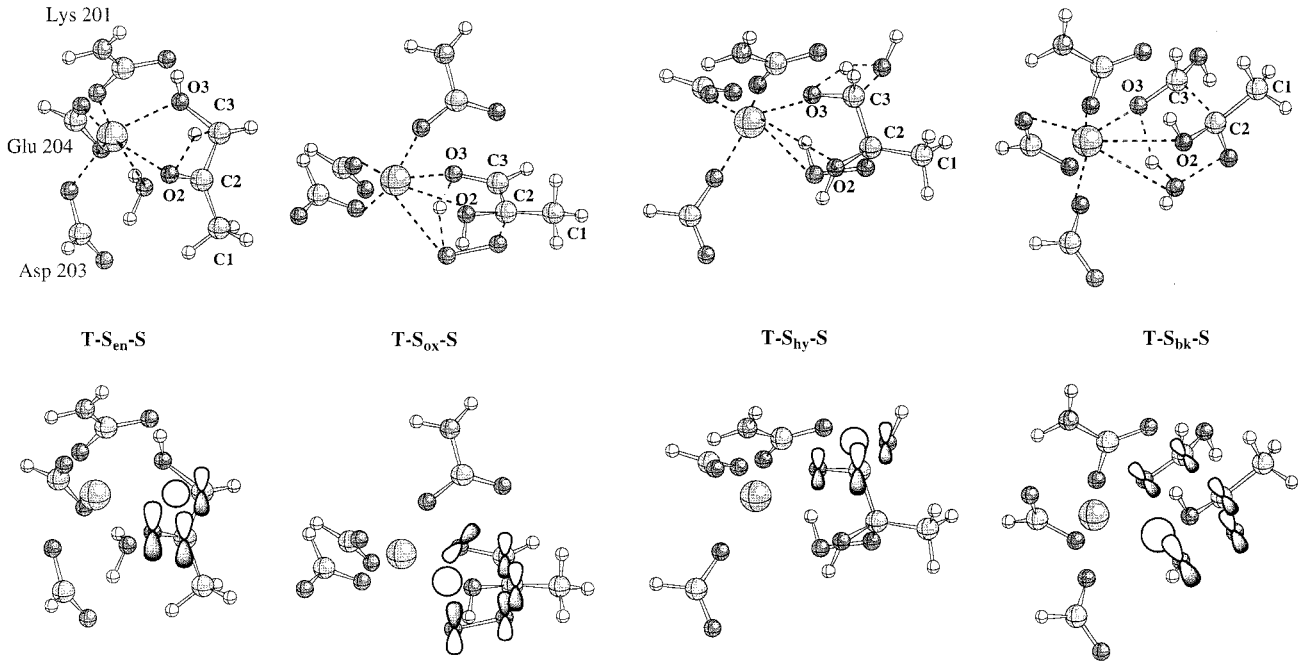

Figure 2. T-Ss obtained for the three-carbon model in a coordination sphere of magnesium. Dashed lines represent bonds that are being broken/formed or coordination interactions between the magnesium ion and its ligands. In the lower row, the structures are sketched with the orbitals engaged in the electronic mechanism.

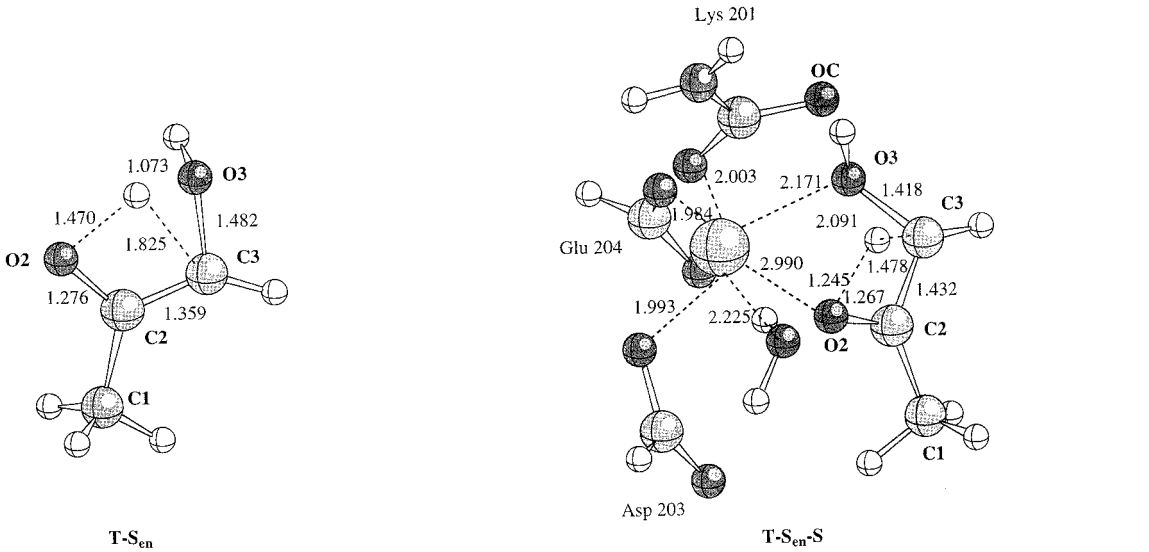

Figure 3. T-S for the enolization step: T-S$_{en}$ (three-carbon model modeling the isolated reactants)[46] and T-S$_{en}$-S (model including the magnesium coordination sphere). Some distances in angstroms, calculated at the HF/6-31G** level, are indicated. Dashed lines represent bonds that are being broken/formed or coordination interactions between the magnesium ion and its ligands.

the MMM. This might be a way to detect fine-tuning catalytic effects to be contrasted with structurally based mechanisms as well as those derived from kinetic measurements. As there are some contradictory views among these latter, the present theoretical study may be useful in this respect by giving a fully independent description of the mechanism.

Transition Structures and Mechanism

The set of transition structures is portrayed in Figure 2. They are calculated with the model including the magnesium coordination sphere. Observe that they can be put in a one-to-one relation with those depicted in Figure 1. This result is remarkable because it was believed that Mg and the other atoms in the coordination shell would impeach the hydrogen shuttling characteristic of the isolated transition structures.

The ligands to Mg define two hemispheres: one has permanent protein residues, while the other coordinates the oxygen atoms from RuBP and eventually a water molecule. In the X-ray structure of 2-CABP, the distances in angstroms are 2.28 (Asp-203), 2.23 (Glu-204), and 2.36 (carbamylated Lys 201); for the inhibitor in the X-ray structure they are 2.37 for O2−Mg and 2.36 for O3−Mg.[42] In the transition structures a meaningful difference between hemispheres appears to be the case (cf. Figure 3), as the substrate's oxygen atoms are at a slightly larger distance than those of the side chains; conventionally, the former occupy the upper hemisphere while the protein side chains occupy the lower hemisphere. In view of the functionality changes from alcohol to ketone during catalysis, the large distance found in the T-S reflects the intermediate nature of these atoms. The lower hemisphere is not only

TABLE 1: Geometric Parameters[a] Calculated for the Indicated T-Ss at the Calculation Level Shown

	HF/3-21G		HF/6-31G**		B3LYP[b]
	T-S_{en}	T-S_{en}-S	T-S_{en}	T-S_{en}-S	T-S_{en}-S
C3−O3	1.516	1.469	1.482	1.418	1.431
C2−C3	1.353	1.418	1.359	1.432	1.428
C2−O2	1.308	1.320	1.276	1.267	1.298
H−C3	1.901	1.501	1.825	1.478	1.475
H−O2	1.508	1.327	1.470	1.245	1.308
H−O3	1.086	2.010	1.073	2.091	2.086
O2−C2−C3−O3	−4.83	−58.54	−4.57	−64.34	−61.93
	T-S_{ox}	T-S_{ox}-S	T-S_{ox}	T-S_{ox}-S	T-S_{ox}-S
C2−O1(O_2)	1.529	1.504	1.458	1.501	1.594
O1(O_2)−O2(O_2)	1.507	1.522	1.421	1.429	1.405
H3−O3	1.068	1.084	1.034	1.072	1.040
H3−O2(O_2)	1.466	1.454	1.471	1.362	1.635
C2−C3	1.466	1.432	1.465	1.454	1.464
C3−O3	1.306	1.332	1.281	1.332	1.324
O2−C2−C3−O3	−20.44	−19.86	−23.00	−16.62	−11.43
	T-S_{hy}	T-S_{hy}-S	T-S_{hy}	T-S_{hy}-S	T-S_{hy}-S
C3−O(H_2O)	1.591	1.570	1.566	1.535	1.613
O3−H1(H_2O)	1.402	1.442	1.342	1.355	1.404
H1(H_2O)−O(H_2O)	1.129	1.111	1.121	1.111	1.122
C3−O3	1.366	1.391	1.320	1.347	1.361
C2−C3	1.493	1.499	1.510	1.511	1.524
O2−C2−C3−O3	−73.06	−71.10	−71.74	−71.19	−69.67
	T-S_{bk}	T-S_{bk}-S	T-S_{bk}	T-S_{bk}-S	T-S_{bk}-S
C2−C3	1.844	1.828	1.731	1.711	1.647
O1(O_2)−O2(O_2)	1.799	1.811	1.810	1.847	1.809
H1(H_2O)−O3	1.527	1.713	1.575	1.757	1.500
H1(H_2O)−O2(O_2)	1.049	0.993	1.009	0.964	1.084
C2−O1(O_2)	1.330	1.302	1.305	1.279	1.323
C2−O2	1.401	1.384	1.369	1.339	1.362
C3−O3	1.274	1.294	1.264	1.282	1.339
O2−C2−C3−O3	−39.74	−44.78	−39.90	−45.59	−48.24

[a] Distances are given in angstroms; dihedral angles are given in degrees. [b] B3LYP stands for B3LYP/6-31G**.

somewhat more crowded than the upper one but is fairly static (there would only be thermal atom fluctuations and not in- and outfluxes of molecules). The local mechanistic action takes place at the upper hemisphere.

The time-dependent projection of transition vectors (normal mode animation) shows fluctuations equivalent to the isolated model with no steric hindrance to the incumbent hydrogen motion. From the structural side, the superposition of carbon frames indicates a fairly good invariance with respect to the effects of the magnesium system. The transition vectors describe fairly localized systems even for the enolization step where the carbamylated lysine plays a fundamental structural role.

Enolization. In Figure 3, the isolated T-S_{en} and that in the Mg sphere (T-S_{en}-S) are depicted. In Table 1, geometric parameters are listed for the three levels of theory used.

The isolated T-S_{en} was early found by us[46,55] and shown to be invariant with model size (compare with the corresponding T-S in Figure 1) and electronic methodology with which it was calculated. The important amplitude in the transition vector gives the displacement of the hydrogen that was bound to C3. The distance H−C3 is large, 1.8−1.9 Å. In view of the transition vector amplitudes, one may suspect in this case a first step, a 1,2-hydrogen migration (from C3 to O3) continued by the T-S_{en}. This vector is dominated by the hydrogen fluctuation between O3 and O2. The atomic frame O2−C2−C3−O3 (the corresponding dihedral angle will be referred to with the Greek letter α) is almost planar, and the hydrogen stands roughly on the same plane. The C2−C3 bond in the T-S_{en} is short (1.35−1.36 Å), reflecting a dienol-like structure. This latter is found as a successor complex. The precursor is unstable compared to the C3−H bond so that an IRC-like (intrinsic reaction coordinate of Fukui[57]) displacement from T-S leads to the correct reactant.

The Mg coordination sphere introduces important qualitative changes in the transition structure. The basic feature, transfer of the hydrogen from C3 to O2, is now neat. The global conformation measured with the dihedral angle α and the transition vector presents significant changes. From $\alpha \approx -5°$ in T-S_{en} down to $\alpha \approx -60°$ in T-S_{en}-S, one can sense the importance of magnesium binding and carbamylated lysine effects. This latter makes a hydrogen bond with the H−O3 hydroxyl group of the substrate.

The transition vector now describes the local fluctuation of the hydrogen being transferred from C3 to O2; this result is independent of the calculation level. The interaction of this hydrogen with O3 is weaker than the one found for the isolated system (the distance changes from 1.1 Å in the T-S_{en} up to 2.1 Å in the T-S_{en}-S). This time O3 is engaged in interactions with magnesium (the distance Mg−O3 is ≈2.1 Å). Furthermore, the carbamate model oxygen atom OC interacts with O3 via hydrogen bonding: the corresponding O3−OC distance is 2.5−2.7 Å, and H−OC, 1.5−1.7 Å.

The T-S_{en}-S provides a possible explanation for the role of the Lys201 that, in our model, would be hydrogen-bonding stabilization and modulation of the isolated T-S. This result agrees with experiment[58,59] in the sense that without this interaction the qualitative nature of the saddle point changes. But there is an important difference in what it has been proposed[15,60] as a role for Lys 201, namely, a proton-abstracting base along enolization.

A quantum chemical analysis of this step has been reported by King et al.[61] There, an intermolecular process is proposed in which the metal-stabilized carbamate of Lys 201 acts also as the base that abstracts the C3 proton, while Lys 175 would play the role of an acid. The role of Lys 175 looks somewhat puzzling, because it has also been proposed that it acts as a base.[15] From Andersson's structure,[60] it is apparent that the Lys 175 is an important element of the phosphate binding site. And, as shown by the work of Lundqvist and Schneider,[62] subtle changes at the phosphate binding site may lead to inactivation for reasons not directly related to its acid−base role in the chemical steps. The fact that mutation of Lys 175 impairs enolization can be understood in part on the basis of the present work and in part on the X-ray work on 2-CABP−Rubisco.[42] If the substrate molding were not sufficient, the activation barrier would increase rendering the enolization step highly unlikely. This would explain the inactivation induced by mutation of Lys 175 rather than its acid activity proposed by one group of researchers[61] or its activity as a base by another.[15]

The geometry results can be supplemented with electronic analyses. The value of the dihedral angle α indicates that the π-bond of the 2,3-enediol is almost broken. This bond would have resulted from the dangling orbital (see Figure 2) left behind by the hydrogen migration from C3, and a p_π orbital at C2. In the reactant, this p_π orbital is engaged with a p_π orbital from O2, forming a π C2═O2 bond. This bond must be broken first. In fact, the hydrogen shuttled from C3 in the T-S_{en}-S would break the π-bond in the carbonyl function C2═O2, thereby engaging a rotated pπ orbital at O2 (orbital steering) to form a σ bond with the hydrogen. This description would be fully consistent if all the bond breaking/forming were homolytic.

Methodologically, homolytic processes are badly described at the Hartree−Fock level of theory, independently of the orbital

SCHEME 1: Relative Energies of the Indicated Species[a]

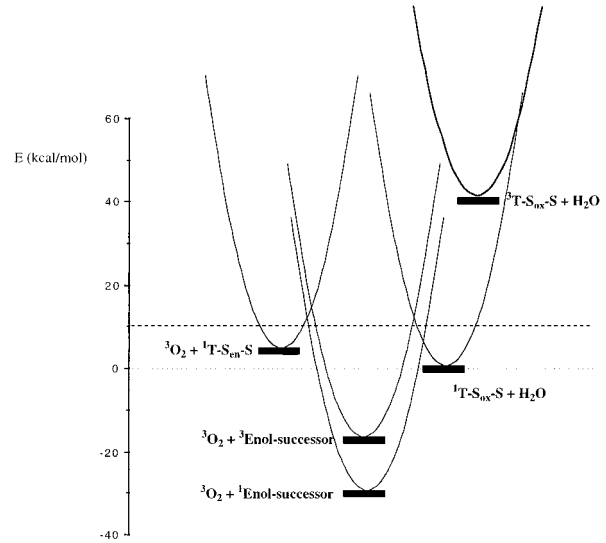

[a] Energies are relative to ^{1}T-S$_{ox}$-S plus a water molecule, in kilocalories per mole, calculated at the HF/3-21G level. The generic parabolas are drawn as a reminder that each species has vibrational modes that must be populated. The dashed line accounts for the existence of the zero-point vibrational energy of ^{1}T-S$_{ox}$-S plus a water molecule.

basis set. A highly correlated level of theory would give a more realistic description of the barriers and electronic distribution. However, the system used here is too large to use multiconfiguration SCF complete active-space methods.[63] Density functional theory-based calculations yield a clearer picture of bond breaking/forming processes.

Not surprisingly, the B3LYP results show large correlation effects. Since the dihedral $\alpha \approx -60°$ would break the π-bonding pattern, a local diradical nature for this bond is a first hint on the nature of the electronic processes. The B3LYP/6-31G** enolization T-S yields a 72% of the charge at the transferred hydrogen, -0.1 and -0.5 excess charge at C3 and O2 atoms, respectively. This would portray a homolytic process of bond breaking/forming instead of a proton transfer.

The result is that no double bond between C2 and C3 is found in the T-S$_{en}$-S. It follows as a conclusion that the standard description of an enediol structure is not in agreement with the present model. Because $\alpha \approx -60°$, the successor complex derived from the T-S$_{en}$-S may open the intersystem crossing channel by acting as reactant in the following step. This angle is found in the 2-CABP−enzyme complex, and we assume that the role of the binding site including magnesium is to keep the successor complex geometry around this value with some degree of structural fluctuation. Thus, the idea that the enolization step must follow a pathway with a large absolute value for this angle becomes reasonable. The 2,3-enediol proposed in the literature is transformed into a 2,3-twisted diol, thereby preparing the C2 center to be attacked by O_2. The same line of argument is valid for carboxylation. The inevitability axiom is understandable in the present approach as it reflects an electronic effect localized in the activated substrate.

Oxygen Binding and Intersystem Crossing. The oxygen molecule has spin-forbidden interactions with singlet-state molecules. One would expect that somehow RuBP substrate should prompt for an activation mechanism. Furthermore, it is widely accepted that when O_2 interacts with the substrate, it is already enolized at the active site. Then, we can take as starting point (see Scheme 1) the T-S$_{en}$-S (whose lower energy fundamental spin state is singlet) plus oxygen molecule $^3O_2$ (which is in a triplet state) and make a "thought experiment". The pair, $^3O_2$ + ^{1}T-S$_{en}$-S, at long distance is in a global triplet electronic state, while the reaction products are all spin singlet states. It is obvious that an intersystem crossing should happen and our problem is to detect when and how this process may take place. Consider the simplest calculation level (HF/3-21G) to make some comparisons.

Let us compare first the energy of T-S for oxygenation, ^{1}T-S$_{ox}$-S, and the corresponding oxygenation T-S in the triplet state (^{3}T-S$_{ox}$-S). This latter is well above the singlet (a difference of about 40 kcal/mol has been found by means of a single point calculation). We conclude that the intersystem crossing would take place before the system populates the singlet oxygenation transition structure.

The energy of the system ^{1}T-S$_{en}$-S plus $^3O_2$ is about 4 kcal/mol above the ^{1}T-S$_{ox}$-S plus a water molecule. This latter is the energy reference in Scheme 1. The energy of $^3O_2$ plus the enolization T-S successor in its singlet electronic state (^{1}enol-successor) is located ca. 30 kcal/mol below the reference. For the same geometry, the $^3O_2$ + ^{3}enol-successor energy is located only 17 kcal/mol below the reference. These two triplet molecules ($^3O_2$ and ^{3}enol-successor) can interact along the reactive path and produce a molecular complex, say $^3O_2$---^{3}enol-successor. The spin space is now enlarged. Note that changes of local orbital angular momentum are involved: the π-bond between C2 and C3 is almost broken, and a π-bond in the O−O system must also be broken to activate the system. Now, two structures having triplet spin states can be decomposed into singlet, triplet, and quintet states. Then, from $^3O_2$---^{3}enol-successor, there is a finite probability to populate the singlet states. The energy states of the ($^3O_2$---^{1}enol-successor) are embedded in those belonging to the ($^3O_2$---^{3}enol-successor). An intersystem crossing that is assisted by local changes of orbital angular momentum would explain the spin conversion. It is apparent that this latter complex would correspond to a possible precursor complex of the oxygenation T-S, leading to the final ^{1}T-S$_{ox}$-S + ^1H_2O. This provides the structural reason for the presence of the ^{3}enol-successor complex. The angle α must be in a vicinity of $\pm 90°$ rather than 0° at the (putative) enediol (or at enol-successor). Fluctuations in a neighborhood of 90° will ensure a near zero singlet−triplet electronic state energy gap as we showed some time ago with dihydroxyethylene,[54,55] thereby increasing the spin state dimension.

Oxygen Fixation Step. According to the above discussion, oxygenation reaction should be carried out in a singlet spin state. In the oxygenation pathway, one obtains the T-Ss for oxygenation, T-S$_{ox}$ and T-S$_{ox}$-S, shown in Figure 4. Geometric parameters are listed in Table 1. A water molecule is displaced by oxygen at Mg coordination shell and, for the time being, it is no longer considered in the present model.

Andrews and Lorimer[17] have proposed that, at any given CO_2/O_2 ratio, the fractional partitioning of RuBP between the carboxylation and oxygenation pathways is dictated by the reactivity of the enzyme-bound 2,3-enediol toward CO_2 and O_2. The conditions required for intersystem crossing and the T-S$_{en}$ strongly suggest not a 2,3-enediol but a 2,3-twisted diol. The attack of CO_2 or O_2 is made onto the same C2 position of the twisted diol.

At variance with the enolization transition structure, the atoms in the coordination shell do not affect the geometry and transition vector of oxygen fixation. The carbon frames are very similar in space orientation. There is a hydrogen exchange at the entrance channel from the hydroxyl group at C3 toward the

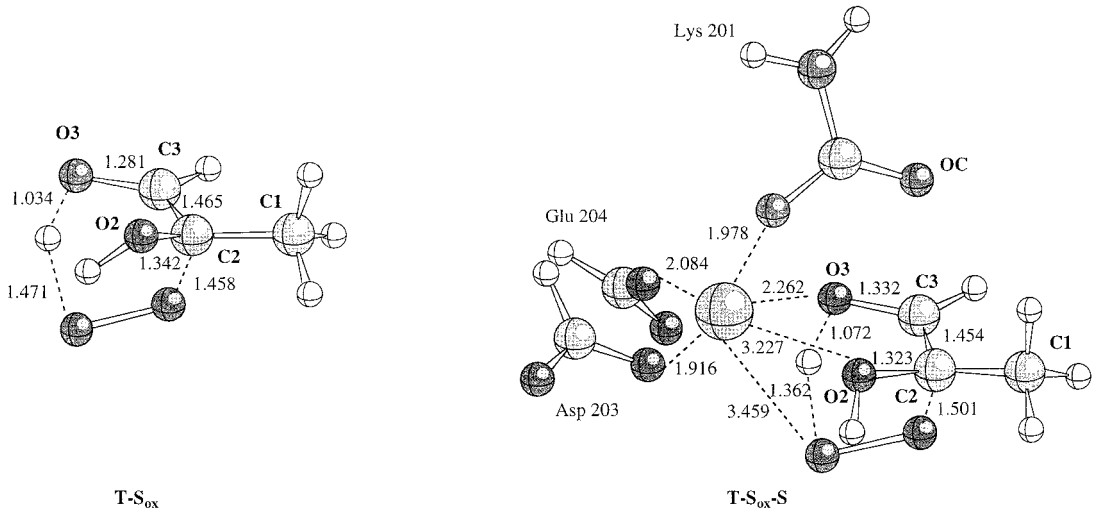

Figure 4. T-S for the oxygenation step: T-S_{ox} (three-carbon model modeling the isolated reactants)[36,37] and T-S_{ox}-S (model including the magnesium coordination sphere). Some distances in angstroms, calculated at the HF/6-31G** level, are indicated.

entering attacking molecule. A carbonyl group is prompted and activated at C3. This results in a hydroxyperoxide moiety, H−O−O^-. At variance with the standard mechanism (cf. Figure 1), there is no need for an external base to abstract the hydrogen of the hydroxyl group at C3. The results show invariance of the hydrogen exchanged between the C3-hydroxyl and the gas reactant O_2. This exchange appears without any impediment from Mg or any other coordinated residue. The T-S is associated with the incorporation of the corresponding gaseous molecule, while the system has already suffered an intersystem crossing as discussed above. This species describes the formation of the new bond to C2 with concomitant hydrogen shift from O3 to one of the gaseous substrate oxygens (H−O−O---C2).

From the simple electronic description, the previous transition structure left a dangling bond at C2 (see Figure 2). To form a σ bond with one of the oxygen atoms, the π-bond must be broken (orbital steering). This is actually done by the hydrogen atom from O3−H. This hydrogen has a 2-fold effect on the reactivity. For one, it breaks the oxygen−oxygen π-bond, thereby prompting the attack of the nonhydrogenated oxygen on to the C2 dangling bond. For the other, the dangling bond left behind at O3 is used to form the local π-bond with the dangling orbital at C3.

Water Attack Process. The direction into which a water molecule may attack C3 is determined by the stereochemistry of both enolization and oxygenation at the coordination shell of the metal. The upper hemisphere is filled with water and the substrate's oxygen, the positions of which are in reasonable agreement with the corresponding atoms in 2-CABP. After oxygen binding, one oxygen from O−O displaces the water molecule bound to Mg. This molecule moves away and the hydrogenated peroxy end (H−O−O) will occupy its position when the system populates the successor complex related to T-S_{ox}-S. In the successor complex, before hydration, the hydrogenated oxygen enters the coordination shell and the displaced water molecule may approach the carbonyl function at C3. Then, in the hydration step, the water molecule enters from the same side as O_2. In view of the subtle electronic processes leading to oxygenation, it is apparent that, for the present model, the hydration cannot be simultaneous with oxygenation. This result was early derived from kinetic and isotope labeling studies for the carboxylation chemistry.[18,64] In view of the present study, this conclusion may also apply to oxygenation.

Therefore, cis-out-of-plane conformation of the O2−C2−C3−O3 fragment and the position of the carbamylated lysine 201 in the crowded Mg shell would prompt the attack of water from the same side as the O_2 did in the previous step. This situation would prevent an attack from the other side assumed in other mechanisms.[15] The metal and its coordination sphere play an important role here in directing the molecular traffic.

Hydration Transition Structure. For hydration at the C3 center, one can see that the corresponding carbonyl group is there available when the oxygenation successor complex, molded into the geometry enforced by the active site, becomes populated. The T-S_{hy} and T-S_{hy}-S structures (Figure 5 and Table 1) are obtained for the oxygenation pathway. These hydration T-Ss are four-member rings, corresponding to concerted mechanisms such that oxygen addition to C3 and hydrogen transfer to the carbonyl oxygen are accomplished in a single step. This type of transition structure has early been found in related hydration of carbonyl compounds.[65] The T-Ss in Figure 5 are similar with respect to geometrical parameters. Even more, the inclusion of the Mg coordination sphere does not prevent hydrogen transfer from the incoming water molecule to O3. The idea that the metal may prevent these types of intramolecular hydrogen transfer is not granted.

A difference can be sensed here in the way hydration is viewed by other workers. The usual mechanistic proposals[15,60,61,66] involve hydroxide ion attack on C3, with one of the water hydrogen atoms sequestered either by His294 or by His327 prior to water oxygen addition to C3. This leads to an overcharged substrate and active-site residue. In the present model, no additional electrostatic charges need to be accumulated and separated on the active site due to the hydration step.

The successor complex, molded into a tense conformation when compared to the fully geometry-optimized species in a vacuum, can prompt for the next stage of the global chemistry. The related product (albeit geometrically deformed) is the equivalent to structure III in Figure 1. This time, however, the hydrogenated peroxide forms a strong hydrogen bond with the carbonyl oxygen at C3 (O3−HOO 1.5−1.8 Å). To yield the final products, all elements are present since another T-S becomes accessible via intramolecular hydrogen transfer.

C2−C3 and O−O Bond Cleavage Step. The pathway leading to the C2−C3 bond breaking uses the molded successor complex corresponding to the *aci*-acid intermediate. The cor-

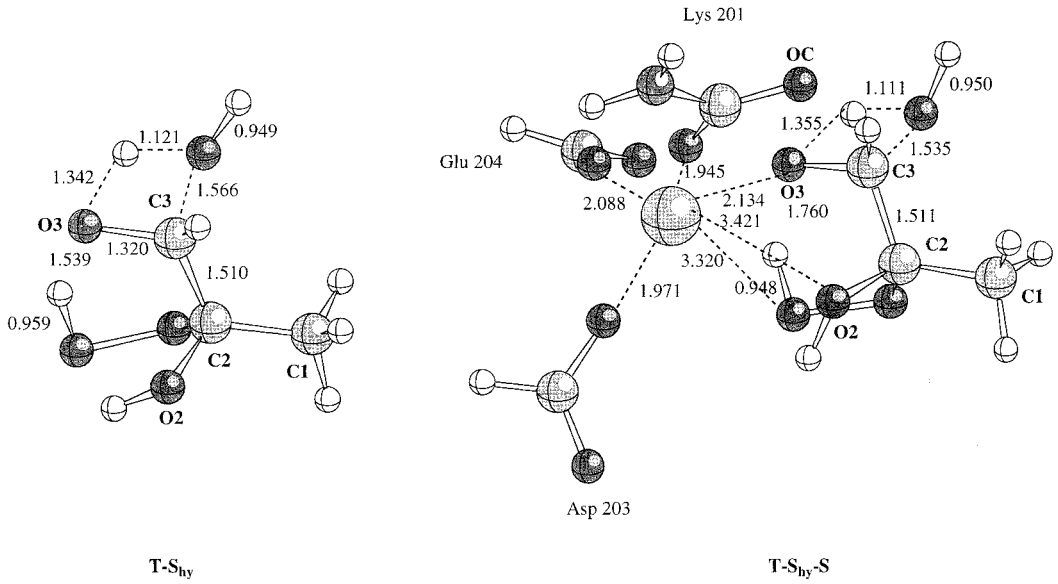

T-S$_{hy}$ **T-S$_{hy}$-S**

Figure 5. T-S for the hydration step within the oxygenation sequence: T-S$_{hy}$ (three-carbon model modeling the isolated reactants)[36,37] and T-S$_{hy}$-S (model including the magnesium coordination sphere). Some distances in angstroms, calculated at the HF/6-31G** level, are indicated.

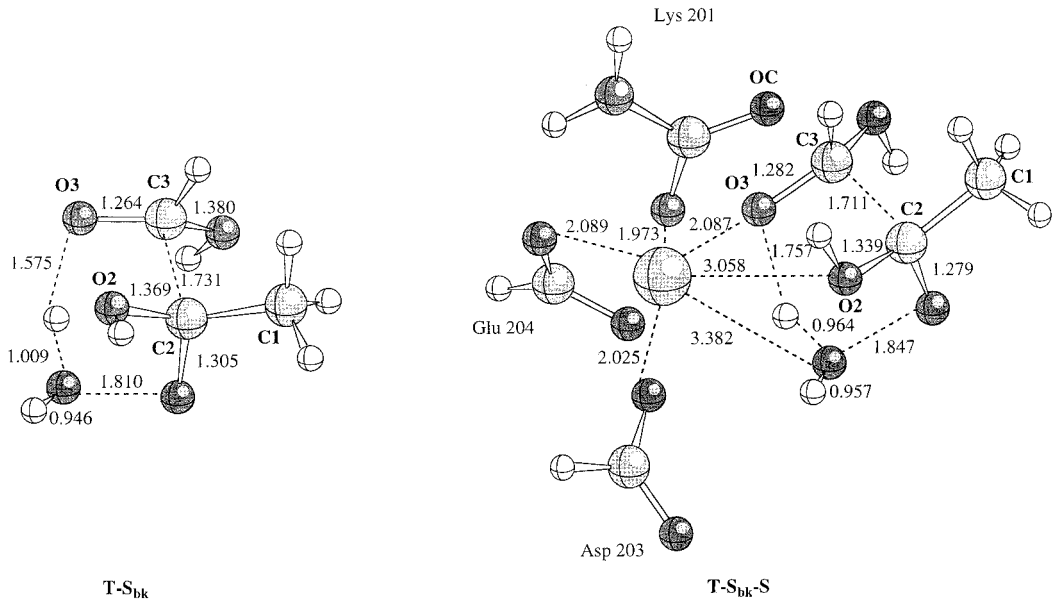

T-S$_{bk}$ **T-S$_{bk}$-S**

Figure 6. T-S for the C2−C3 bond cleavage step within the oxygenation sequence: T-S$_{bk}$ (three-carbon model modeling the isolated reactants)[36,37] and T-S$_{bk}$-S (model including the magnesium coordination sphere). Some distances in angstroms, calculated at the HF/6-31G** level, are indicated.

responding transition structures are T-S$_{bk}$ and T-S$_{bk}$-S (cf. Figure 6 and Table 1).

The C2−C3 bond breaks concomitantly with an intramolecular hydrogen transfer process in the reactive sequence. The carbon−carbon cleavage has been a puzzling feature when coming to a theoretical explanation of the mechanism. The final bond-breaking (bk) transition structures T-S$_{bk}$ and T-S$_{bk}$-S (Figure 6) correspond to simultaneous C2−C3 and O−O bond-breaking processes. One of the hydrogen atoms of the water molecule from the previous step is transferred to the hydrogenated oxygen of the peroxide, forming a new water molecule. This water molecule can remain coordinated to the Mg^{2+}. The energy used to dehydrate the metal is recovered at this stage. Thus, one oxygen atom of $^3O_2$ is transformed into solvent as experimentally required,[18] and this water molecule is formed as solvent coordinated to the metal. This simplifies the commonly accepted mechanism by eliminating the hydronium ion intermediate.

Mechanism: Experiment and Theory

The set of transition structures and precursor and successor complexes calculated with the magnesium coordinated system yields a comprehensive mechanistic view. This view can be correlated with experimental experience available for the real system. Only the most important aspects are highlighted.

(1) Experimentally, Rubisco is capable of catalyzing a whole set of reactions one after another,[16] and many intermediates in the Rubisco reaction are sufficiently stable that they can be isolated and later fed back to the enzyme, enabling the kinetic study of individual steps. The kinetics can be interpreted as a Theorell-Chance type in which oxygen adds to the enediol of RuBP in a bimolecular fashion after abstraction of the C-3 hydrogen of the sugar bisphosphate. The theoretical results agree to a large extent, albeit some important changes must be considered. The T-Ss are concatenated by precursor−successor linking two different steps, thereby producing a sequentially ordered description. The initial RuBP molding followed by

enolization would prompt for all subsequent processes. This result depends on the carbamylated lysine in our model. The important thing is to realize that labeling isotope studies for the C3−H hydrogen transfer would give support to the present conclusion (see point 3). Moreover, the present enolization mechanism differs from the common accepted view and still is capable of a consistent description.

(2) It was determined that the substrate bound to the activated Rubisco has a definite orientation.[67] For a real enzyme, this goes without saying. The theoretical results for enolization and oxygenation transition structure documents this point in a model where the full enzyme is absent. This suggests that substrate molding is one of the activating mechanisms. The transition structures fit the active site without problem.

(3) Rubisco catalyzes the appearance of solvent tritium at C3 of RuBP.[68] This was interpreted as a proof of the enediol (or enediolate) intermediate and also as evidence that the C3 proton has to move to a place where exchange with solvent hydrogen is possible. The theoretical results agree with this hydrogen motion, although from the present side, there is a twisted diol instead of a enediol. The oxygenation reaction requires a triplet state to activate oxygen as discussed here, and this is achieved with the help of the carbamylated lysine. The standard carbanion theory requires an external general acid and base catalyst to get around with the proton traffic. The molding theory advanced here has a wider scope in the sense that a general explanation can be obtained including the source of intersystem crossing. If the enolization step were the rate-limiting step, from the transition vector of T-S_{en}-S, one would conclude that there was a deuterium isotope effect in the global kinetics.

(4) Indirect evidence seems to prove the existence of a peroxy intermediate in the oxygenation process.[56,69] The theoretical identification of the hydroxyperoxy structure in the transition structure of oxygenation and the corresponding successor complex fully agree with this hypothesis.

(5) The oxygenation products are 3-PGA and 2-PG.[70,71] No configuration inversion at C2 is needed in this case (2-PG lacks asymmetric carbons) as was the case in carboxylation. The T-S_{bk}-S offers a clear explanation to this process. The process appears to be linked to the fate of the oxygen atoms from the gaseous oxygen. This has been experimentally established[71,72] and the theoretical results fully agree with them.

(6) Site-directed mutant species have been used to investigate possible roles for active-site residues. The absence of the carbamylated Lys 201 prevents enolization and formation of a six-carbon intermediate in the RuBP carboxylation chemistry. In view of the key role played by the carbamate in the present model, the theoretical results give further support to the paramount catalytic role played by this residue. On the other hand, mutation of Lys 175 severely impairs enolization and carboxylation;[73,74] mutation of Lys 334 reduces the CO_2/O_2 specificity of the enzyme.[75] The results can be interpreted now from the present point of view. Substrate molding is one key element. The molding critically depends on precise substrate binding. Any mutated residue that affects the result of substrate molding may modify either or both activities. For instance, the role of isoleucine 164 and asparagine 111 (*R. rubrum*) studied by Chène et al.[76,77] can also be interpreted from the substrate molding perspective.

Another important result concerns the nature of the oxygen−protein complex. Oxygen $^3O_2$, due to its spin state, does not interact strongly with any portion of the protein. To do this, a second triplet state is required. Therefore, no standard Michaelis complex can be expected. The T-Ss clearly indicate that this gas substrate can only bind via intersystem crossing with the activated (enolized) substrate RuBP. The kinetic mechanism of Rubisco was described as a modified Theorell-Chance mechanism, and the process is sequentially ordered: RuBP binds first and oxygen then reacts by second-order kinetics with the activated intermediate without first forming a Michaelis complex.[64,76] The agreement of the theoretical results with the kinetic mechanism is then quite satisfactory.

Final Remarks

The present theoretical study correlates to a very reasonable extent with the kinetic and structural information of Rubisco's catalytic mechanism. The concatenated elementary steps can be viewed as mediated by a set of intramolecular hydrogen arrangements, with the absence of direct acid−base catalysis by active-site side chains. According to the proposed intramolecular mechanism, the coordination shell residues are left, at the end of the catalytic cycle, as they were at the beginning, without conventional acid−base catalysis and without any traffic from outside into the active site. Once the loop 6 (spinach structure) is open,[5] the products may diffuse toward the solution, the active site is left in the same state as it was, and a new catalytic cycle can take place.

The quantum calculations have introduced some important features of the active site but not all the residues thought to intervene during catalysis. These residues may be supporting substrate binding and its productive molding. These two latter factors are also fundamental for the theoretical representation of catalysis. The protein is there to bind the substrates. However, the substrate must be molded so that the nuclei would fluctuate around the geometry space defined by the transition structures. The idea is based upon the geometry invariance of a given T-S to interactions with the surroundings. The comparison of geometry between the stationary structure with and without magnesium for the processes of oxygenation, hydration, and final C−C and O−O bond breaking clearly suggests geometry invariance. The electronic structure and T-Ss geometry are properties of the reactive subsystem elicited as stationary saddle points of index one. The partial exception seems to be the enolization step. Here, the active-site model carbamylated Lys 201 residue plays a fundamental role in contributing to a geometry deformation that would prompt the interaction of oxygen with the enolization successor structure. This is a theoretical landmark for the unusual catalytic properties of this system. Enolization is an intramolecular redox process, and in the present context it is also a mechanism to electronically activate the C2 center together with the C3 center. The intersystem crossing is assisted by the successor complex geometry around the C2−C3 axis. In turn, this provides a binding site for the $^3O_2$.

The structural information gathered for the transition-state analogue, CABP, at the active site clearly suggests that the molecular events can take place in the way derived from the theoretical study. The fact that this enzyme can catalyze so many chemical steps can be traced to the relative invariance of the carbon framework found of the transition structures controlling the chemistry. The stationary geometry of each one of the different T-Ss differs among each other but they are all lying within the configuration space allowed by the active site. Such is also the case for the elementary steps calculated for self-inhibition.[4]

The substrate molding has also an important catalytic consequence: a role of the transferred hydrogen atom appears

to be a way to induce orbital steering. As the electronic structure must change from carbonyl to alcohol, for instance, or from C2−C3 π-bond to broken π-bond, the orbital structure must be changed. The processes are facilitated by the proximity of the donor−acceptor groups in the molded conformation of reactants. In fact, these changes of orbital angular momentum (L) together with the expanded spin space (S) produced by torsion of O2−C2−C3−O3 dihedral suggest that it is the $L + S = J$ angular momentum which actually controls the intersystem crossing process. To change spin, the system uses changes in orbital angular momentum. One of the main factors involved in catalysis appears to be the ability of transforming protein−substrate binding energy into a driving force molding the substrate into a geometric space characteristic of the transition structure of model reactions in a vacuum.

Acknowledgment. O.T. is an Iberdrola Foundation invited visiting professor at Jaume I University. This work was supported by research funds of the DGICYT (Project PB96-0795-C02-02). Calculations were performed on two Silicon Graphics Indigo 2 R10000 workstation of the Departament de Ciències Experimentals and on two Silicon Graphics Power Challenger L of the Servei d'Informàtica of the Universitat Jaume I. We are indebted to these centers for providing us with computer capabilities. M.O. thanks the Ministerio de Educación y Ciencia and Jaume I University for FPI fellowships. O.T. thanks Iberdrola Foundation (Spain) and NFR (Sweden) for financial support.

References and Notes

(1) Fersht, A. *Enzyme structure and mechanism*, 2nd ed.; W. H. Freeman & Co.: New York, 1985.
(2) Jordan, D. B.; Chollet, R. *J. Biol. Chem.* **1983**, *258*, 13752.
(3) Edmonson, D. L.; Kane, H. J.; Andrews, T. J. *FEBS Lett.* **1990**, *260*, 62.
(4) Tapia, O.; Andrés, J.; Safont, V. S. *J. Phys. Chem.* **1996**, *100*, 8543.
(5) Schneider, G.; Lindqvist, Y.; Brändén, C.-I. *Annu. Rev. Biophys. Biomol. Struct.* **1992**, *21*, 119.
(6) Andrews, T. J.; Hatch, M. D. *Biochem. J.* **1969**, *114*, 117.
(7) Laing, W. A.; Christeller, J. T. *Biochem. J.* **1976**, *159*, 563.
(8) McCurry, S. D.; Pierce, J.; Tolbert, N. E.; Orme-Johnson, W. H. *J. Biol. Chem.* **1981**, *249*, 6623.
(9) Sicher, R. C.; Hatch, A. L.; Stumpf, D. K.; Jensen, R. G. *Plant Physiol.* **1981**, *68*, 252.
(10) Mott, K. A.; Berry, J. A. *Plant Physiol.* **1986**, *82*, 77.
(11) Robinson, S. P.; Portis, A. R., Jr. *Plant Physiol.* **1989**, *90*, 968.
(12) Yokota, A.; Kitaoka, S. *Plant Cell Physiol.* **1989**, *30*, 183.
(13) Lee, E. H.; Harpel, M. R.; Chen, Y.-R.; Hartman, F. C. *J. Biol. Chem.* **1993**, *268*, 26583.
(14) Hartman, F. C.; Harpel, M. R. *Annu. Rev. Biochem.* **1994**, *63*, 197.
(15) Cleland, W. W.; Andrews, T. J.; Gutteridge, S.; Hartman, F. C.; Lorimer, G. H. *Chem. Rev.* **1998**, *98*, 549.
(16) Miziorko, H. M.; Lorimer, G. H. *Annu. Rev. Biochem.* **1983**, *52*, 507.
(17) Andrews, T. J.; Lorimer, G. H. In *The biochemistry of plants*; Hatch, M. D., Ed.; Academic Press: Orlando, FL, 1987; Vol. 10.
(18) Schloss, J. V. In *Enzymatic and model carboxylation and reduction reactions for carbon dioxide utilization*; Aresta, M., and Schloss, J. V., Eds.; Kluwer Academic Publishers: Dordrecht, The Netherlands, 1990.
(19) Lorimer, G. H.; Andrews, T. J. *Nature* **1973**, *243*, 359.
(20) Pauling, L. *Nature* **1948**, *161*, 707.
(21) Tapia, O.; Cárdenas, R.; Andrés, J.; Colonna-Cesari, F. *J. Am. Chem. Soc.* **1988**, *110*, 4046.
(22) Eklund, H.; Plapp, B. V.; Samama, J.-P.; Brändén, C.-I. *J. Biol. Chem.* **1982**, *257*, 14349.
(23) Tapia, O. *J. Mol. Catal.* **1988**, *47*, 199.
(24) Stanton, R. V.; Peräkylä, M.; Bakowies, D.; Kollman, P. *J. Am. Chem. Soc.* **1998**, *120*, 3448.
(25) Lightstone, F. C.; Zheng, Y.-J.; Bruice, T. C. *J. Am. Chem. Soc.* **1998**, *120*, 5611.
(26) Warshel, A.; Levitt, M. *J. Mol. Biol.* **1976**, *103*, 227.
(27) Warshel, A. *Curr. Opin. Struct. Biol.* **1992**, *2*, 230.
(28) Oliva, M.; Safont, V. S.; Andrés, J.; Tapia, O. *J. Phys. Chem. A* **1999**, *103*, 8725.
(29) Moliner, V.; Turner, A. J.; Williams, I. H. *J. Chem. Soc., Chem. Commun.* **1997**, 1271.
(30) Turner, A. J.; Moliner, V.; Williams, I. H. *Phys. Chem. Chem. Phys.* **1999**, *1*, 1323.
(31) Tapia, O.; Poulain, E.; Sussman, F. *Chem. Phys. Lett.* **1975**, *33*, 65.
(32) Tapia, O.; Goscinski, O. *Mol. Phys.* **1975**, *29*, 1653.
(33) Tapia, O.; Johannin, G. *J. Chem. Phys.* **1981**, *75*, 3624.
(34) Tapia, O.; Andrés, J.; Safont, V. S. *J. Chem. Soc., Faraday Trans.* **1994**, *90*, 2365.
(35) Moliner, V.; Andrés, J.; Oliva, M.; Safont, V. S.; Tapia, O. *Theor. Chem. Acc.* **1999**, *101*, 228.
(36) Oliva, M.; Safont, V. S.; Andrés, J.; Tapia, O. *Chem. Phys. Lett.* **1998**, *294*, 87.
(37) Oliva, M.; Safont, V. S.; Andrés, J.; Tapia, O. *J. Phys. Chem. A* **1999**, *103*, 6009.
(38) Safont, V. S.; Oliva, M.; Andrés, J.; Tapia, O. *Chem. Phys. Lett.* **1997**, *278*, 291.
(39) Andrés, J.; Oliva, M.; Safont, V. S.; Moliner, V.; Tapia, O. *Theor. Chem. Acc.* **1999**, *101*, 234.
(40) Tapia, O.; Oliva, M.; Safont, V. S.; Andrés, J. *Chem. Phys. Lett.* **2000**, *323*, 29.
(41) Tapia, O.; Andrés, J.; Safont, V. S. *J. Mol. Struct. THEOCHEM* **1995**, *342*, 131.
(42) Andersson, I. *J. Mol. Biol.* **1996**, *259*, 160.
(43) Mezey, P. G. *Theor. Chim. Acta (Berlin)* **1980**, *54*, 95.
(44) Mezey, P. G. *Potential energy hypersurfaces*; Elsevier: Amsterdam, 1987.
(45) Tapia, O.; Andrés, J. *Chem. Phys. Lett.* **1984**, *109*, 471.
(46) Tapia, O.; Andrés, J.; Safont, V. S. *J. Phys. Chem.* **1994**, *98*, 4821.
(47) McIver, J. W. *Acc. Chem. Res.* **1974**, *7*, 72.
(48) McIver, J. W., Jr.; Komornicki, A. *J. Am. Chem. Soc.* **1972**, *94*, 2625.
(49) Schlegel, H. B. *J. Chem. Phys.* **1982**, *77*, 3676.
(50) Schlegel, H. B. *J. Comput. Chem.* **1982**, *3*, 214.
(51) Frisch, M. J.; Trucks, G. W.; Schlegel, H. B.; Gill, P. M. W.; Johnson, B. G.; Robb, M. A.; Cheeseman, J. R.; Keith, T.; Petersson, G. A.; Montgomery, J. A.; Raghavachari, K.; Al-Laham, M. A.; Zakrzewski, V. G.; Ortiz, J. V.; Foresman, J. B.; Cioslowski, J.; Stefanov, B. B.; Nanayakkara, A.; Challacombe, M.; Peng, C. Y.; Ayala, P. Y.; Chen, W.; Wong, M. W.; Andres, J. L.; Replogle, E. S.; Gomperts, R.; Martin, R. L.; Fox, D. J.; Binkley, J. S.; Defrees, D. J.; Baker, J.; Stewart, J. P.; Head-Gordon, M.; Gonzalez, C.; Pople, J. A. GAUSSIAN 94; Gaussian, Inc.: Pittsburgh, PA, 1995.
(52) Frisch, M. J.; Trucks, G. W.; Schlegel, H. B.; Scuseria, G. E.; Robb, M. A.; Cheeseman, J. R.; Zakrzewski, V. G.; Montgomery, J. A., Jr.; Stratmann, R. E.; Burant, J. C.; Dapprich, S.; Millam, J. M.; Daniels, A. D.; Kudin, K. N.; Strain, M. C.; Farkas, O.; Tomasi, J.; Barone, V.; Cossi, M.; Cammi, R.; Mennucci, B.; Pomelli, C.; Adamo, C.; Clifford, S.; Ochterski, J.; Petersson, G. A.; Ayala, P. Y.; Cui, Q.; Morokuma, K.; Malick, D. K.; Rabuck, A. D.; Raghavachari, K.; Foresman, J. B.; Cioslowski, J.; Ortiz, J. V.; Baboul, A. G.; Stefanov, B. B.; Liu, G.; Liashenko, A.; Piskorz, P.; Komaromi, I.; Gomperts, R.; Martin, R. L.; Fox, D. J.; Keith, T.; Al-Laham, M. A.; Peng, C. Y.; Nanayakkara, A.; Gonzalez, C.; Challacombe, M.; Gill, P. M. W.; Johnson, B.; Chen, W.; Wong, M. W.; Andres, J. L.; Gonzalez, C.; Head-Gordon, M.; Replogle, E. S.; Pople, J. A. GAUSSIAN 98; Gaussian, Inc.: Pittsburgh, PA, 1998.
(53) GaussView1.0; Gaussian, Inc.: Pittsburgh, PA, 1997.
(54) Andrés, J.; Safont, V. S.; Tapia, O. *Chem. Phys. Lett.* **1992**, *198*, 515.
(55) Andrés, J.; Safont, V. S.; Queralt, J.; Tapia, O. *J. Phys. Chem.* **1993**, *97*, 7888.
(56) Harpel, M. R.; Serpersu, E.; Lamerdin, J. A.; Huang, Z.-H.; Gage, D. A.; Hartman, F. C. *Biochemistry* **1995**, *34*, 11296.
(57) Fukui, K. *J. Phys. Chem.* **1970**, *74*, 4161.
(58) Smith, H. B.; Larimer, F. W.; Hartman, F. C. *Biochem. Biophys. Res. Commun.* **1988**, *152*, 579.
(59) Lorimer, G. H.; Gutteridge, S.; Madden, M. W. *Partial reactions of ribulose bisphosphate carboxylase: their utility in the study of mutant enzymes*; Plenum Press: New York, 1988.
(60) Taylor, T. C.; Andersson, I. *J. Mol. Biol.* **1997**, *265*, 432.
(61) King, W. A.; Gready, J. E.; Andrews, T. J. *Biochemistry* **1998**, *37*, 15414.
(62) Lundqvist, T.; Schneider, G. *J. Biol. Chem.* **1989**, *264*, 7078.
(63) Roos, B. J. In *Lecture notes in quantum chemistry*; Roos, B. J., Ed.; Springer-Verlag: Berlin, 1992; Vol. 58.
(64) Van Dyk, D. E.; Schloss, J. *Biochemistry* **1986**, *25*, 5145.
(65) Spangler, D.; Williams, I. H.; Maggiora, G. M. *J. Comput. Chem.* **1983**, *4*, 524.
(66) Newman, J.; Gutteridge, S. *J. Biol. Chem.* **1993**, *268*, 25876.

(67) Lorimer, G. H.; Gutteridge, S.; Reddy, G. S. *J. Biol. Chem.* **1989**, *264*, 9873.
(68) Saver, B. G.; Knowles, J. R. *Biochemistry* **1982**, *21*, 5398.
(69) Chen, Y.-R.; Hartman, F. C. *J. Biol. Chem.* **1995**, *270*, 11741.
(70) Bowes, G.; Ogren, W. L.; Hagerman, R. H. *Biochem. Biophys. Res. Commun.* **1971**, *45*, 716.
(71) Lorimer, G. H. *Annu. Rev. Plant. Physiol.* **1981**, *32*, 349.
(72) Lorimer, G. H.; Andrews, T. J.; Tolbert, N. E. *Biochemistry* **1973**, *12*, 18.
(73) Lorimer, G. H.; Hartman, F. C. *J. Biol. Chem.* **1988**, *263*, 6488.
(74) Hartman, F. C.; Soper, T. S.; Niyogi, S. K.; Mural, R. J.; Foote, R. S.; Mitra, S.; Lee, E. H.; Machanoff, R.; Larimer, W. F. *J. Biol. Chem.* **1987**, *262*, 3496.
(75) Gutteridge, S.; Rhoades, D.; Herrmann *J. Biol. Chem.* **1993**, *268*, 7818.
(76) Chène, P.; Day, A. G.; Fersht, A. R. *J. Mol. Biol.* **1992**, *225*, 891.
(77) Chène, P.; Day, A. G.; Fersht, A. R. *Biochem. Biophys. Res. Commun.* **1997**, *232*, 482.